HEAVY ION RESULTS WITH THE ATLAS EXPERIMENT AT THE LHC*

Barbara Wosiek

for the ATLAS Collaboration

The Henryk Niewodniczański Institute of Nuclear Physics
Polish Academy of Sciences
Radzikowskiego 152, 31-342 Kraków, Poland

(Received December 12, 2011)

An overview of the first results on particle production in lead–lead collisions at $\sqrt{s_{NN}} = 2.76$ TeV obtained with the ATLAS detector is presented. The results were obtained from the sample of minimum bias lead–lead collision data from the 2010 LHC run, with an integrated luminosity up to 9 μb^{-1}. The measurements of global and collective features of lead–lead collisions are shown and complemented with studies of high-transverse momentum probes, including charged hadron suppression, jet quenching, dijet energy imbalance and di-lepton final states.

DOI:10.5506/APhysPolB.43.507
PACS numbers: 25.75.–q, 25.75.Gz, 25.75.Ld

1. Introduction

In the fall 2010, the Large Hadron Collider (LHC) at CERN delivered lead–lead collisions at the energy of $\sqrt{s_{NN}} = 2.76$ TeV, fourteen times higher than the energy available from the Relativistic Heavy Ion Collider (RHIC) at BNL. This opened a new era in the field of ultra-relativistic heavy ion physics, providing a unique opportunity for the study in detail the properties of the created hot and dense matter.

The ATLAS detector [1], designed for studying high-transverse momentum phenomena in proton–proton collisions, is well suited to perform a wide spectrum of measurements in the dense environment of heavy ion collisions. It consists of three main subsystems: the inner detector, the calorimetry and

* Presented at the Conference "Strangeness in Quark Matter 2011", Kraków, Poland, September 18–24, 2011.

the muon spectrometer, all with a full coverage in azimuth. The inner detector, placed in a 2 T solenoid magnetic field, allows for precise determination of charged particle trajectories over a pseudorapidity range up to $|\eta| = 2.5$. The finely segmented calorimetric system provides energy measurements, both electromagnetic and hadronic, over almost 10 units of pseudorapidity. The outermost muon spectrometer provides triggering, identification and precise momentum measurements for muons produced with $|\eta| < 2.7$.

The data sets used in the analyses presented here correspond to up to 8 μb^{-1} of minimum bias lead–lead collisions taken with the solenoid field on and about 1 μb^{-1} recorded with the solenoid switched off. The total transverse energy measured in the ATLAS forward calorimeters (FCal, covering $3.2 < |\eta| < 4.9$) is used to estimate the collision centrality. The centrality intervals are expressed in percentiles of the total inelastic lead–lead cross section with an estimated sampling fraction of $98 \pm 2\%$. For each centrality class the number of participating nucleons, $\langle N_{\rm part}\rangle$, and the number of binary nucleon–nucleon collisions, $\langle N_{\rm coll}\rangle$ are evaluated with a Monte Carlo Glauber calculations using simulated total transverse energy in FCal [2].

2. Initial state characterization

Global event properties, such as the total charged particle multiplicity and collective flow phenomena, determine the initial properties of the created hot, dense system. Particle multiplicity is proportional to the entropy of the initial system and can be used to estimate the initial gluon density. Collective flow phenomena, measured via the azimuthal anisotropy of produced particles, are sensitive to the conditions of the system at the very early stage of its evolution and are crucial for constraining the initial geometric configuration of nucleons from the colliding nuclei.

The measurement of the charged particle multiplicity was performed on the data with solenoid magnet turned off, using three layers of the ATLAS pixel detector, within $|\eta| < 2$ [3]. Three reconstruction methods have been applied. The first two use two-point tracklets, formed by hits on two pixel layers and constrained by the reconstructed primary vertex, with applied different procedures for controlling the level of fake tracklets. The third method uses the three-point tracks reconstructed with the ATLAS tracking software. The measured $dN_{\rm ch}/d\eta/(\langle N_{\rm part}\rangle/2)$, averaged over $|\eta| < 0.5$ for the 0–6% centrality interval, of $8.5 \pm 0.1(\text{stat.}) \pm 0.4(\text{syst.})$ is consistent with the ALICE [4] and CMS [5] results as shown in the left panel of Fig. 1. The charged particle yield per participant pair increases by a factor of two relative to RHIC data. Centrality dependence of the charged particle density per participant pair is plotted as a function of $\langle N_{\rm part}\rangle$ in the right panel of Fig. 1. We observe a good agreement with the ALICE and CMS for all centrality intervals down to the most peripheral collisions. When compared to the

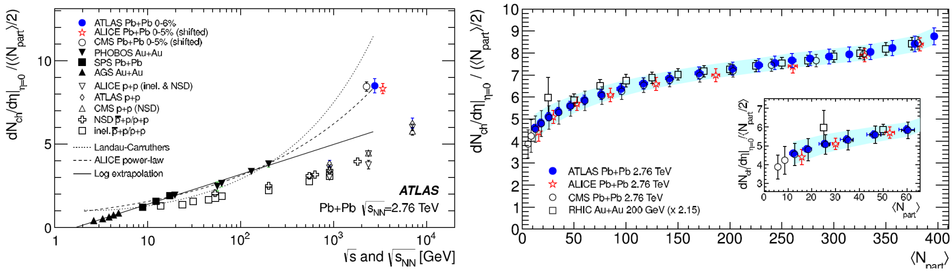

Fig. 1. (Left) Energy dependence of the charged particle density per colliding nucleon pair measured by ATLAS for 6% of the most central collisions and averaged over $|\eta| < 0.5$, compared to other heavy ion results as well as the measurements of the charged particle density in proton(antiproton)–proton collisions. (Right) Centrality dependence of $dN_{\mathrm{ch}}/d\eta/(N_{\mathrm{part}}/2)$ compared with ALICE and CMS data as well as RHIC data multiplied by 2.15 to allow comparison with the $\sqrt{s_{NN}} = 2.76$ TeV results. The inset shows in more detail results for $\langle N_{\mathrm{part}}\rangle$ below 60.

top energy RHIC data multiplied by 2.15, it can be seen that centrality dependence of the charged particle density scales with the beam energy, indicating that it is predominantly geometric in its origin.

Collective flow, which manifests itself as a large anisotropy in the event-by-event azimuthal angle distribution of produced particles, is a consequence of the spatial anisotropy of the initial overlap region of the colliding nuclei. Initial spatial anisotropies are converted into final state momentum anisotropies via strong rescattering processes which induce pressure gradients. Anisotropic flow is commonly studied by measuring the Fourier coefficients (v_n) of the azimuthal angle distributions of the emitted particles. The second harmonic, v_2, referred to as elliptic flow, is the most extensively studied as it most directly relates the anisotropic shape of the overlap of the colliding nuclei to a corresponding anisotropy of the outgoing momentum distribution. Higher order Fourier harmonics are sensitive to fluctuations in the initial spatial deformation [6]. In ATLAS, Fourier harmonics are measured with the event plane method [7] and two-particle correlation [8] methods. The event plane angle, Ψ_n, is measured in the forward calorimeters, FCal $3.2 < |\eta| < 4.9$ while the flow harmonics, $v_n = \langle\cos(n[\phi - \Psi_n])\rangle$ are determined using azimuthal angles (ϕ) of charged particles reconstructed in the inner detector over $|\eta| < 2.5$ [2, 9].

Figure 2 shows the dependence of v_2 on p_{T} for transverse momenta from 0.5 up to 20 GeV measured in $|\eta| < 1$ in eight centrality intervals. A strong p_{T} dependence is observed with a rapid rise up to p_{T} of about 3 GeV, then a decrease up to about 8–10 GeV, followed by a weak dependence at the highest transverse momenta. It was shown [2] that at high transverse momenta v_2

seems to be independent of the beam energy. It remains to be seen whether this energy scaling is consistent with the predictions of models describing the parton energy loss in a dense, hot medium. The pseudorapidity dependence of v_2 was studied over $|\eta| < 2.5$ and shows a very weak dependence, much weaker than that observed at the RHIC energy.

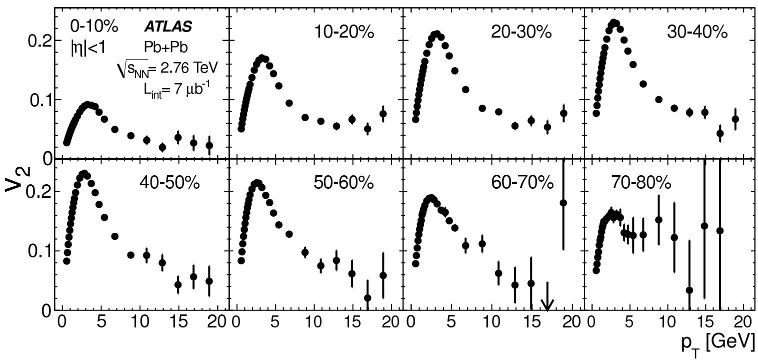

Fig. 2. Elliptic flow as a function of p_T for eight 10% centrality intervals, for p_T from 0.5 to 20 GeV and for $|\eta| < 1$.

Higher Fourier harmonics, up to $n = 6$ are shown in Fig. 3 [9]. It can be seen that only v_2 shows a significant centrality dependence, while higher order coefficients show no centrality dependence, indicating that the latter are sensitive to the fluctuations in the initial spatial deformations, while v_2 measures the shape of the overlap region.

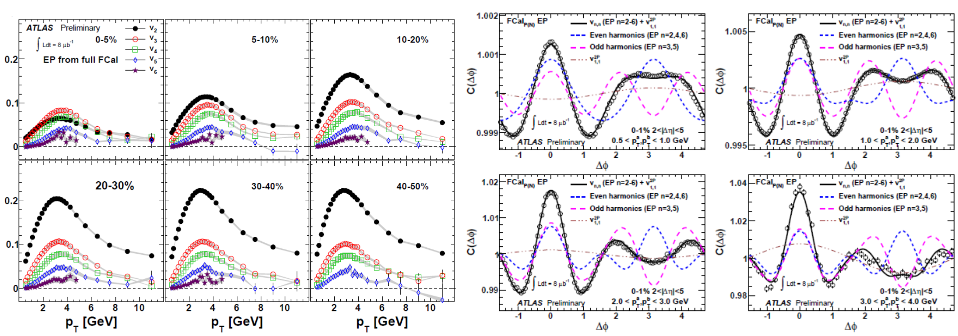

Fig. 3. (Left) Higher order flow harmonics ($n = 2$–6) as a function of p_T for eight 10% centrality intervals, for p_T from 0.5 to 20 GeV and for $|\eta| < 1$. (Right) Comparison of the measured two-particle correlation function and the correlation function reconstructed from the v_2–v_6 Fourier coefficients obtained with the event plane method and v_1 from the two-particle correlations for 1% of the most central collisions in four different transverse momentum ranges.

Flow harmonics were also measured with the two-particle correlation method and found to be consistent with that obtained with the event plane method [9]. In addition, it is shown that the rich structure observed in the two-particle correlations, namely the jet peak and ridge on the near-side and two-peak structure on the away-side, can be nicely described by the interplay of different flow coefficients as illustrated in the left panel of Fig. 3. This observation suggests that the structures observed in the two-particle correlation function can not be attributed to the medium response to jets but rather to fluctuations in the initial state geometry and a subsequent collective hydrodynamic-like system evolution.

3. Weakly interacting probes

For the first time at the LHC energy it is possible to study the production of W and Z bosons in heavy ion collisions. This provides us with weakly interacting probes which should be insensitive to the properties of the created medium. In ATLAS these measurements are done via bosons decays to muon final states: $Z \to \mu^+\mu^-$, $W^\pm \to \mu^\pm\nu$. The production yield of Z bosons is measured by requiring two muons with invariant mass in the range from 66 to 116 GeV [10]. Altogether 38 Z candidates are observed with a negligible background level. The W production yields are obtained by fitting the muon transverse momentum spectra with a template describing the p_{T} shape of muons from simulated W decays and a parameterized function to account for muons from heavy flavor quark decays [11]. A sample of about 400 W bosons is obtained. Figure 4 shows in the left panel the centrality dependence of R_{CP} defined as the Z yield measured in a certain centrality interval normalized to the yield measured in peripheral 40–80% centrality interval with all yields scaled by the corresponding num-

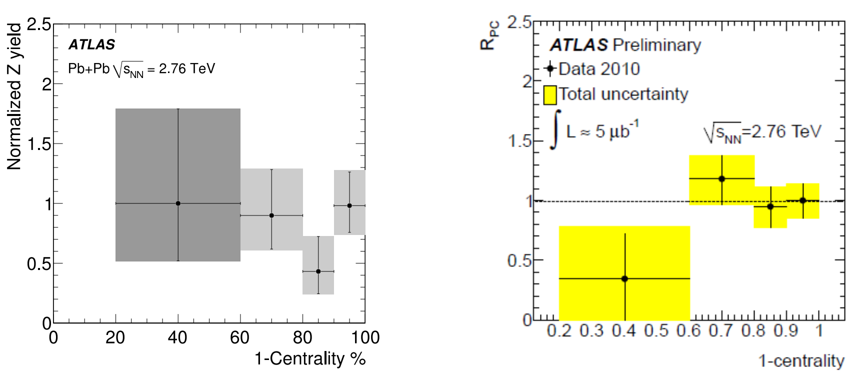

Fig. 4. (Left) Centrality dependence of the Z yields normalized to the yield measured in peripheral collisions with all yields scaled by the corresponding number of binary nucleon–nucleon collisions. (Right) The same as on the left panel for W yields normalized to the most central collisions.

ber of binary nucleon–nucleon collisions. The right panel shows similar data for W bosons with yields in this case normalized to the yield measured in 10% of the most central collisions. Due to the limited statistics it is not possible to draw definite conclusions, but it seems that the Z yields scale with the number of binary collisions. For Ws, the fit to constant value gives 0.99 ± 0.10 with a $\chi^2 = 3.02$ for three degrees of freedom, showing that the centrality dependence of Ws yields is consistent with binary collision scaling. As expected, electroweak boson yields are not affected by the medium. Much higher statistics are needed to fully exploit the rich physics potential in the sector of electroweak bosons, which includes in particular constraining the nuclear modification of the parton distribution function or using weakly interacting bosons produced in association with jets to get a good understanding of the parton energy loss in the medium.

4. Medium-sensitive probes

As shown above electroweak bosons produced in heavy ion collisions obey the expected scaling of yields with the number of binary collisions. This is not the case for probes produced initially in high-transfer momentum processes, which are sensitive to the conditions prevailing at the early collision times. Then, typically the suppression of yields is expected, quantified by deviations from the binary collision scaling.

Suppression of heavy quarkonia states was predicted and observed for J/Ψ at RHIC [12] and SPS [13] energies. Counter-intuitively, the level of suppression was found to be independent of the collision energy, although the initial system conditions strongly vary with the energy. At the LHC, the J/Ψ suppression similar to that observed at RHIC is also reported [10]. The left panel of Fig. 5 shows the ATLAS measurement of $R_{\rm CP}$ for J/Ψ yields

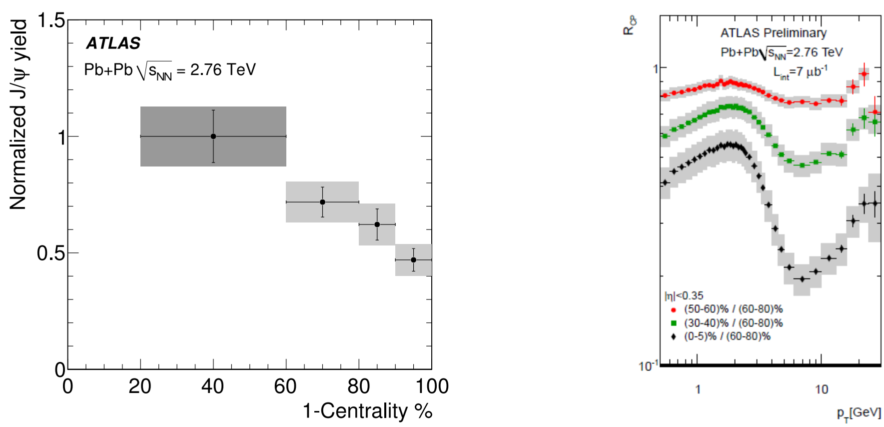

Fig. 5. (Left) Centrality dependence of the J/Ψ $R_{\rm CP}$. (Right) Single hadron $R_{\rm CP}$ as a function of transverse momentum for three centrality intervals.

obtained via dimuon decays where the 40–80% peripheral centrality interval is used for normalization. One can see that normalized yields do not follow the binary collision scaling, but show a significant decrease from peripheral to central collisions.

The suppression is also observed for charged hadrons. In ATLAS, charged hadrons have been measured out to 30 GeV [14]. The measured transverse momentum dependence of $R_{\rm CP}$ is shown in the right panel of Fig. 5 for three centrality classes and pseudorapidity ranges specified on the plot. One can see that $R_{\rm CP}$ for most central collisions stays significantly below one out to 30 GeV in transverse momentum. This clear deviation from the binary collision scaling, also reported at RHIC energy, provides indirect evidence for the jet quenching phenomenon, the process by which energetic partons lose energy traversing through the hot, dense medium. This energy loss can occur through radiative emission of gluons, collisional energy loss due to elastic scattering, or a variety of other processes.

The study of jet quenching phenomenon is the LHC domain, and the ATLAS detector with highly segmented large acceptance calorimeters has excellent capabilities for reconstructing jets in lead–lead collisions. The inclusive jet production rates, expected to be modified by jet quenching, have been measured for the data sample recorded in 2010 [15]. Jets were reconstructed using the anti-$k_{\rm t}$ algorithm [16] with different size parameters, R, and with the underlying background removed on an event-by-event basis. Figure 6 shows jet $R_{\rm CP}$ (here defined relative to 60–80% centrality interval) as a function of centrality in three fixed jet transverse energy bins ($E_{\rm T}$) for $R = 0.4$ and $R = 0.2$ jets. $R_{\rm CP}$ decreases smoothly from peripheral to cen-

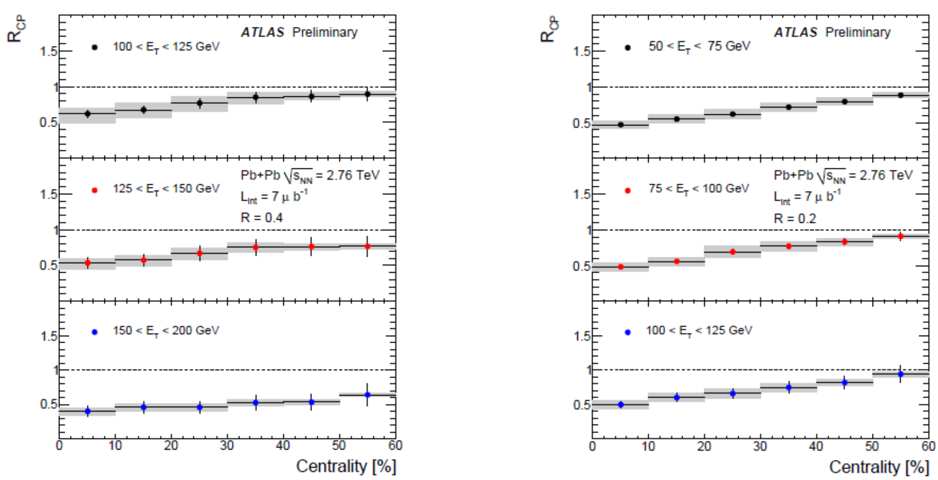

Fig. 6. Jet $R_{\rm CP}$ as a function of centrality (with the most central events on the left) for three $E_{\rm T}$ intervals, and for $R = 0.4$ (left) and $R = 0.2$ (right) jets.

tral collisions. In the most central collisions (0–10%), a suppression by a factor of two is observed for all E_{T} bins and for both jet size parameters. The comparable suppression for $R = 0.4$ and $R = 0.2$ jets is inconsistent with the predictions from calculations of radiative energy loss [17]. These calculations also predict a substantial modification of the jet fragmentation functions [18]. To measure the jet transverse and longitudinal fragmentation functions, the tracks reconstructed in the inner detector with $p_{\mathrm{T}} > 2$ GeV were used to construct the j_{T} — the transverse momentum, and z — the longitudinal momentum fraction of the charged jet constituents relative to the jet axis. Directly measured transverse and longitudinal fragmentation functions do not show substantial variation with the collision centrality. This is illustrated in Fig. 7 which shows the j_{T} and z distributions measured in central 0–10% events and peripheral 40–80% collisions.

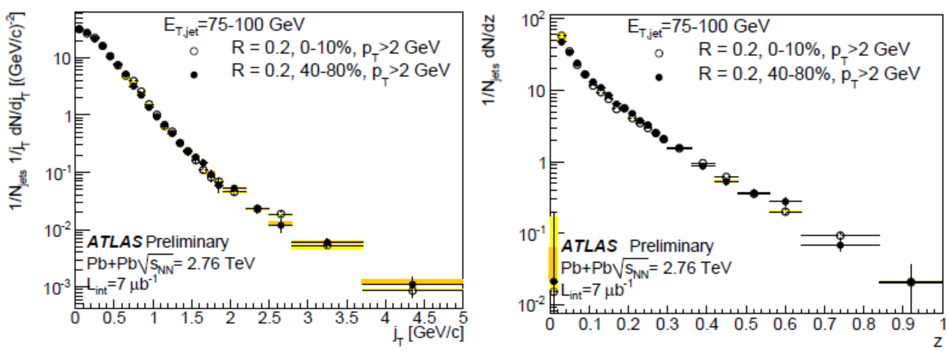

Fig. 7. Comparison of the transverse (left) and longitudinal (right) jet fragmentation functions for central 0–10% events and peripheral 40–80% collisions.

A measurement of a strong energy imbalance in di-jet events was reported by ATLAS using $R = 0.4$ anti-k_{T} jets with a leading jet E_{T1} above 100 GeV and a subleading jet E_{T2} greater than 25 GeV [19]. This measurement provided the first direct evidence for the jet quenching where each jet traversed a different path length in the medium. The di-jet asymmetry is defined as $A_J = (E_{\mathrm{T1}} - E_{\mathrm{T2}})/(E_{\mathrm{T1}} + E_{\mathrm{T2}})$, where E_{T2} is the transverse energy of the highest E_{T} jet emitted in the hemisphere opposite to the leading jet. Here, we report on the same measurement, but using smaller jets ($R = 0.2$) in order to check a possible bias caused by the fluctuations in the underlying event background. The measured distributions [15] are shown in Fig. 8 in six centrality intervals and compared to the same distributions obtained from simulated HIJING events with embedded PYTHIA di-jets. The right panel of Fig. 8 shows the azimuthal angle separation between the two jets. One can see similar broadening of the A_J distribution for central collisions as previously reported for a larger jet size parameter. Jets are predominantly emitted back-to-back, as shown in the right panel of Fig. 8. The observation of the same trends in the di-jet asymmetry for different jet sizes is not consistent with the postulated underlying event fluctuations as an explanation of the measured di-jet asymmetry [20].

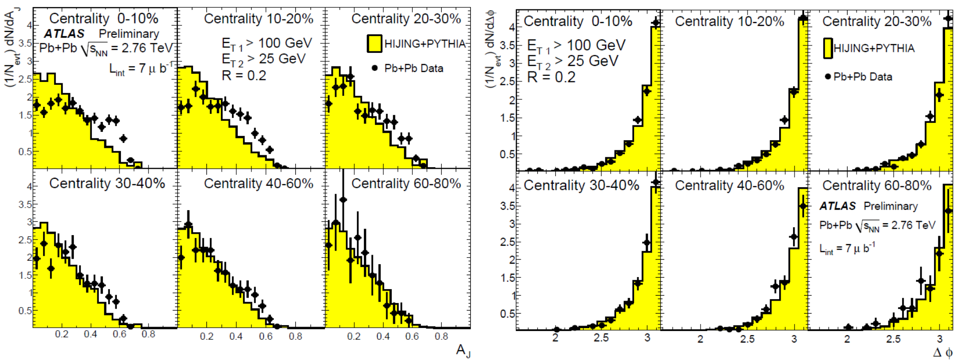

Fig. 8. Di-jet asymmetry (left) and azimuthal angle separation (right) for $R = 0.2$ jets in six centrality intervals, compared to Monte Carlo simulations of HIJING with embedded PYTHIA dijets.

5. Summary

Results are presented for lead–lead collisions at $\sqrt{s_{NN}} = 2.76$ TeV obtained by the ATLAS Collaboration using up to 9 μb^{-1} of integrated luminosity recorded during the 2010 LHC heavy ion run. The charged particle density at mid-rapidity increases by a factor of two relative to the top RHIC energy and shows centrality dependence similar to that measured at RHIC. Elliptic flow, v_2, has been measured over large pseudorapidity and transverse momentum ranges. Transverse momentum dependence of v_2 for charged hadrons is similar to RHIC measurements while much weaker dependence on pseudorapidity is observed at the LHC energy as compared to RHIC data. Higher order flow components have been measured up to v_6 and show little centrality dependence indicating their sensitivity to the fluctuations in the initial geometry. The structures observed in the two-particle correlation functions at low transverse momenta can be described by the interplay of contributions from different flow harmonics, calling into question their interpretation in terms of the jet-medium interactions.

Electroweak boson production is found to be consistent with the binary nucleon–nucleon collision scaling. Contrary, J/Ψ yields show deviations from the binary collision scaling with a strong suppression of the yields in the most central collisions. This suppression is similar to that reported at lower energies, indicating that possibly the mechanism of quarkonia regeneration starts to be more important at high energy collisions. Strong suppression is also observed in the yields of single charged hadrons measured out to p_{T} of 30 GeV.

The first measurements of inclusive jet spectra and jet suppression have been performed. Jets are suppressed in central collisions by a factor of two relative to peripheral events. The suppression shows no significant dependence on the jet transverse energy and is independent of the jet size parameter. The jet fragmentation functions show no substantial modification with increasing collision centrality, both in the transverse and longitudinal jet fragment distributions. The di-jet energy asymmetry distributions measured with smaller jets and thus less susceptible to the underlying background fluctuations show a similar broadening with centrality as previously reported for larger jets.

This work was supported by the Polish Ministry of Science and Higher Education and its grants for Scientific Research.

REFERENCES

[1] ATLAS Collaboration, *JINST* **3**, S08003 (2008).
[2] ATLAS Collaboration, *Phys. Lett.* **B707**, 330 (2012) [arXiv:1108.6018 [hep-ph]].
[3] ATLAS Collaboration, arXiv:1108.6027 [hep-ph].
[4] ALICE Collaboration, *Phys. Rev. Lett.* **106**, 032301 (2011).
[5] CMS Collaboration, *J. High Energy Phys.* **08**, 141 (2011) [arXiv:1107.4800 [nucl-ex]].
[6] B. Alver, G. Roland, *Phys. Rev.* **C81**, 054905 (2010).
[7] A.M. Poskanzer, S.A. Voloshin, *Phys. Rev.* **C58**, 1671 (1998).
[8] K. Adcox *et al.* [PHENIX Collaboration], *Phys. Rev. Lett.* **89**, 212301 (2002).
[9] ATLAS Collaboration, ATLAS-CONF-2011-074.
[10] ATLAS Collaboration, *Phys. Lett.* **B697**, 294 (2011).
[11] ATLAS Collaboration, ATLAS-CONF-2011-078.
[12] A. Adare *et al.* [PHENIX Collaboration], *Phys. Rev. Lett.* **98**, 232301 (2007).
[13] B. Alessandro *et al.* [NA50 Collaboration], *Eur. Phys. J.* **C39**, 335 (2005).
[14] ATLAS Collaboration, ATLAS-CONF-2011-079.
[15] ATLAS Collaboration, ATLAS-CONF-2011-075.
[16] M. Cacciari, G.P. Salam, G. Soyez, *J. High Energy Phys.* **04**, 063 (2008).
[17] I. Vitev, S. Wicks, B.-W. Zhang, *J. High Energy Phys.* **11**, 093 (2008).
[18] N. Armesto *et al.*, *J. High Energy Phys.* **0802**, 048 (2008).
[19] ATLAS Collaboration, *Phys. Rev. Lett.* **105**, 252303 (2010).
[20] M. Cacciari, G.P. Salam, G. Soyez, *Eur. Phys. J.* **C71**, 1692 (2011).